

# Cytokinesis-Block Micronucleus Assay Using Human Lymphocytes as a Sensitive Tool for Cytotoxicity/Genotoxicity Evaluation of AgNPs

Balam Ruiz-Ruiz, María Evarista Arellano-García,\* Patricia Radilla-Chávez, David Sergio Salas-Vargas, Yanis Toledano-Magaña,\* Francisco Casillas-Figueroa, Roberto Luna Vazquez-Gomez, Alexey Pestryakov, Juan Carlos García-Ramos, and Nina Bogdanchikova



Cite This: *ACS Omega* 2020, 5, 12005–12015



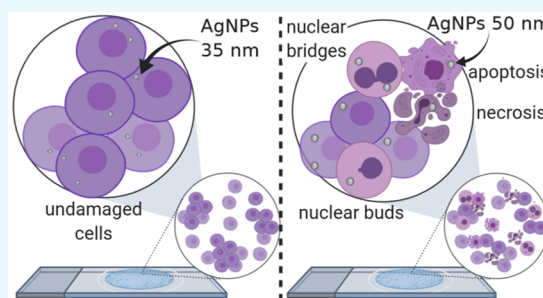
Read Online

ACCESS |

Metrics & More

Article Recommendations

**ABSTRACT:** Silver nanoparticles (AgNPs) are the most used nanomaterials worldwide due to their excellent antibacterial, antiviral, and antitumor activities, among others. However, there is scarce information regarding their genotoxic potential measured using human peripheral blood lymphocytes. In this work, we present the cytotoxic and genotoxic behavior of two commercially available poly(vinylpyrrolidone)-coated silver nanoparticle (PVP–AgNPs) formulations that can be identified as noncytotoxic and nongenotoxic by just evaluating micronuclei (MNi) induction and the mitotic index, but present enormous differences when other parameters such as cytotaxis, apoptosis, necrosis, and nuclear damage (nuclear buds (NBUDs) and nucleoplasmic bridges (NPBs)) are analyzed. The results show that Argovit (35 nm PVP–AgNPs) and nanoComposix (50 nm PVP–AgNPs), at concentrations from 0.012 to 12  $\mu\text{g}/\text{mL}$ , produce no changes in the nuclear division index (NDI) or micronuclei (MNi) frequency compared with the values found on control cultures of human blood peripheral lymphocytes from a healthy donor. Still, 50 nm PVP–AgNPs significantly decrease the replication index and significantly increase cytotaxis, apoptosis, necrosis, and the frequencies of nuclear buds (NBUDs) and nucleoplasmic bridges (NPBs). These results provide evidence that the cytokinesis-block micronucleus (CBMN) assay using human lymphocytes and evaluating the eight parameters provided by the technique is a sensitive, fast, accurate, and inexpensive detection tool to support or discard AgNPs or other nanomaterials, which is worthwhile for continued testing of their effectiveness and toxicity for biomedical applications. In addition, it provides very important information about the role played by the [coating agent]/[metal] ratio in the design of nanomaterials that could reduce adverse effects as much as possible while retaining their therapeutic capabilities.



## INTRODUCTION

Silver nanoparticles (AgNPs) have been widely used in consumer and industrial products and recently in biomedicine, mainly because they exhibit beneficial properties by acting as broad-spectrum antimicrobials, and anti-inflammatory, antiviral, and antitumor agents, among other features.<sup>1–4</sup>

Due to their extensive uses, several concerns have been raised as to whether exposure to AgNPs can produce cytotoxic and genotoxic effects in humans. However, it is difficult to objectively compare the different studies because they include a wide variety of factors such as size, shape, coating, or stabilizers in addition to the diverse biological test models and the biomarkers used to identify toxicity.

Different articles report the cytotoxic and genotoxic effects of AgNPs;<sup>5–13</sup> however, the lack of a systematic model to identify their genotoxic potential makes it hard to make decisions regarding the safety of nanomaterials, mostly when

standard models are used, like the Ames test, which does not provide reliable results.<sup>14</sup>

In this sense, cytokinesis-block micronucleus (CBMN) assay could fulfill this requirement; this technique, recently endorsed by the OECD,<sup>15</sup> is considered one of the most robust methods for assessing cytotoxicity and genotoxicity since it provides nine biomarkers. For cytotoxicity, the cytokinesis-block proliferation index (CBPI) or replication index (RI) and its associated cytotaxis percentage (% Cyt), apoptosis, and necrosis are the biomarkers. The former shows the proliferative

Received: January 12, 2020

Accepted: May 6, 2020

Published: May 21, 2020



capacity of human lymphocytes under the experimental conditions tested. On the other hand, apoptosis and necrosis indicate the number of cells dying through regulated processes or linked to severe damage events that exceed the ability of the cell to repair itself, respectively.<sup>16</sup>

In the case of genotoxicity, frequencies of micronuclei (MNi), nuclear buds (NBUDs), and nucleoplasmic bridges (NPBs) are the biomarkers. MNi, being the product of clastogenic and/or aneugenic processes, are widely described in the literature.<sup>17,18</sup> NBUDs have been described as amplified repair DNA fragments produced in response to damage elicited by reactive oxygen species (ROS) and reactive nitrogen species (RNS), while NPBs are the result of (1) cellular repair processes, (2) poorly matched chromosomes that arise from damage in the mitotic spindle related to inhibitors in the synthesis and repair of DNA, and (3) general chemical agents that break the phosphodiester structure of DNA (Figure 1).<sup>18,19</sup>

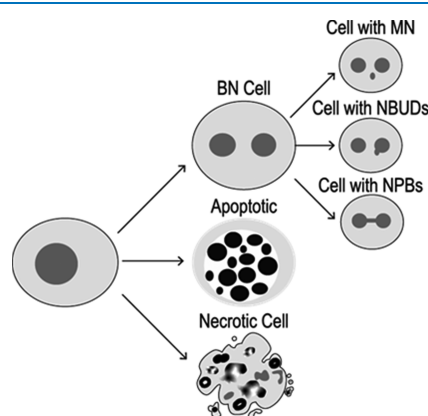


**Figure 1.** Cytotoxic and genotoxic damage that can be tracked by the CBMN assay.

The use of the CBMN assay allowed the authors to emphasize the role of the size, shape, and type of the stabilizer used as a coating agent in the cytotoxic and genotoxic effects observed. To our knowledge, the CBMN assay is nevertheless underused and just a few authors have evaluated the effects of AgNPs with it.<sup>20–22</sup> Furthermore, in practically all of the cases, they find that the silver nanoparticles assessed are cytotoxic and produce genotoxic damage at low concentrations.<sup>23–26</sup>

Overall, it has been observed that AgNP formulations evaluated on human lymphocytes produce genotoxic damage, with an intensified effect produced by the uncoated nanoparticles.<sup>24,26–29</sup> Butler and co-workers found an increase in the number of cells with micronuclei with size and concentration dependencies; the smaller the size of the nanoparticle, the higher the observed percentage of cells with micronuclei and the lower the concentration of nanoparticles needed to produce the effect.<sup>28</sup> Even so, the sensitivity of preserved lines is lower compared with primary cultures as shown by Greulich,<sup>30</sup> a factor that definitely affects the observed genotoxic effect. This difference in cellular sensitivity is one of the main reasons to strongly recommend the use of primary cultures as the first step to determine the cytotoxic and genotoxic damage produced by nanomaterials.

On the other hand, in the last few years, our research group studied an AgNP formulation that has been fully characterized using different physicochemical techniques and applied in

several research areas with outstanding results.<sup>31–40</sup> In Russia, this formulation was approved for use in humans as a nutritional supplement, in cosmetics, and recently in hemostatic sponges in surgery.<sup>32</sup> Its application led to remission of symptoms and re-epithelialization of tissues in the treatment of human otitis.<sup>33</sup> Besides, topical application proved to be useful for the rapid healing of patients with chronic diabetic foot ulcers.<sup>34</sup> This formulation produces a remarkable antiproliferative effect on solid human tumor cell lines,<sup>31</sup> which could be triggered by ROS overproduction. Moreover, we recently found that it reduces tumor growth and increases the lifespan of mice with melanoma more than twofold compared with cisplatin.<sup>41</sup> In veterinary applications, results showed their antiviral effectiveness in treating infectious rhinotracheitis and bovine viral diarrhea,<sup>35</sup> Rift Valley virus in mice,<sup>36</sup> canine distemper,<sup>37</sup> and the white spot syndrome virus (WSSV) in shrimp.<sup>38,42</sup> Our multidisciplinary research group has also published that concentrations of 25 and 50 mg/L of this AgNP formulation are useful as an antibacterial agent for sanitizing the culture media used for micropropagation of plants.<sup>39</sup> Furthermore, at these particular concentrations, it elicits a hormetic effect on high-value commercial crops such as sugar cane and vanilla.<sup>39,40</sup> All of these processes occur without cytotoxic or genotoxic damage to the plant after 6 weeks of exposure.<sup>43</sup>

Due to these findings, our group is focusing on new biomedical applications for this AgNP formulation. Therefore, it is crucial to assess the biocompatibility of this nanomaterial, particularly its genotoxic potential in primary cultures.

This work aims to evaluate the cytotoxic and genotoxic effects of the commercially available AgNP formulation Argovit on peripheral blood human lymphocytes of a healthy donor. It will be done following the CBMN model proposed by the OECD through the evaluation of nine biomarkers.<sup>44</sup> Then, the results will be compared with the findings reported for other AgNPs and other chemicals to evaluate whether the CBMN assay can be proposed as a low-cost technique, reproducible and effective for a first screening of cytotoxic and genotoxic profiles of nanomaterials.

## RESULTS

The measurement of CBPI indicates the cytotoxic effects due to the exposure to different concentrations of the chemical agents assessed. As expected, our results showed that sodium arsenite produces a major decrease in the CBPI ( $1.216 \pm 0.156$ ) compared with the negative control ( $1.500 \pm 0.002$ ). A similar effect was observed for poly(vinylpyrrolidone) (PVP) and 50 nm PVP–AgNPs, with CBPI values in the range of 1.21–1.26 for the former and 1.18–1.36 for the latter. Interestingly, no difference was observed between 35 nm PVP–AgNPs and the control group (Figure 2a). The differences in cellular toxicity elicited by each agent are most evident on analyzing the replication index (RI) (Figure 2b), where 35 nm PVP–AgNPs do not show differences compared with the control; meanwhile, the other evaluated agents decrease it by more than a half, like sodium arsenite, with values of 21.6% and the lowest concentration assayed of 50 nm PVP–AgNPs (0.012  $\mu\text{g}/\text{mL}$ ) that exhibited 36.5%.

The cytostasis induced by each agent clearly shows that sodium arsenite significantly affects the cellular division, the same as PVP at both concentrations evaluated, with more than 50% cytostasis. However, the most relevant result for us was the difference found between both AgNP formulations: 50 nm

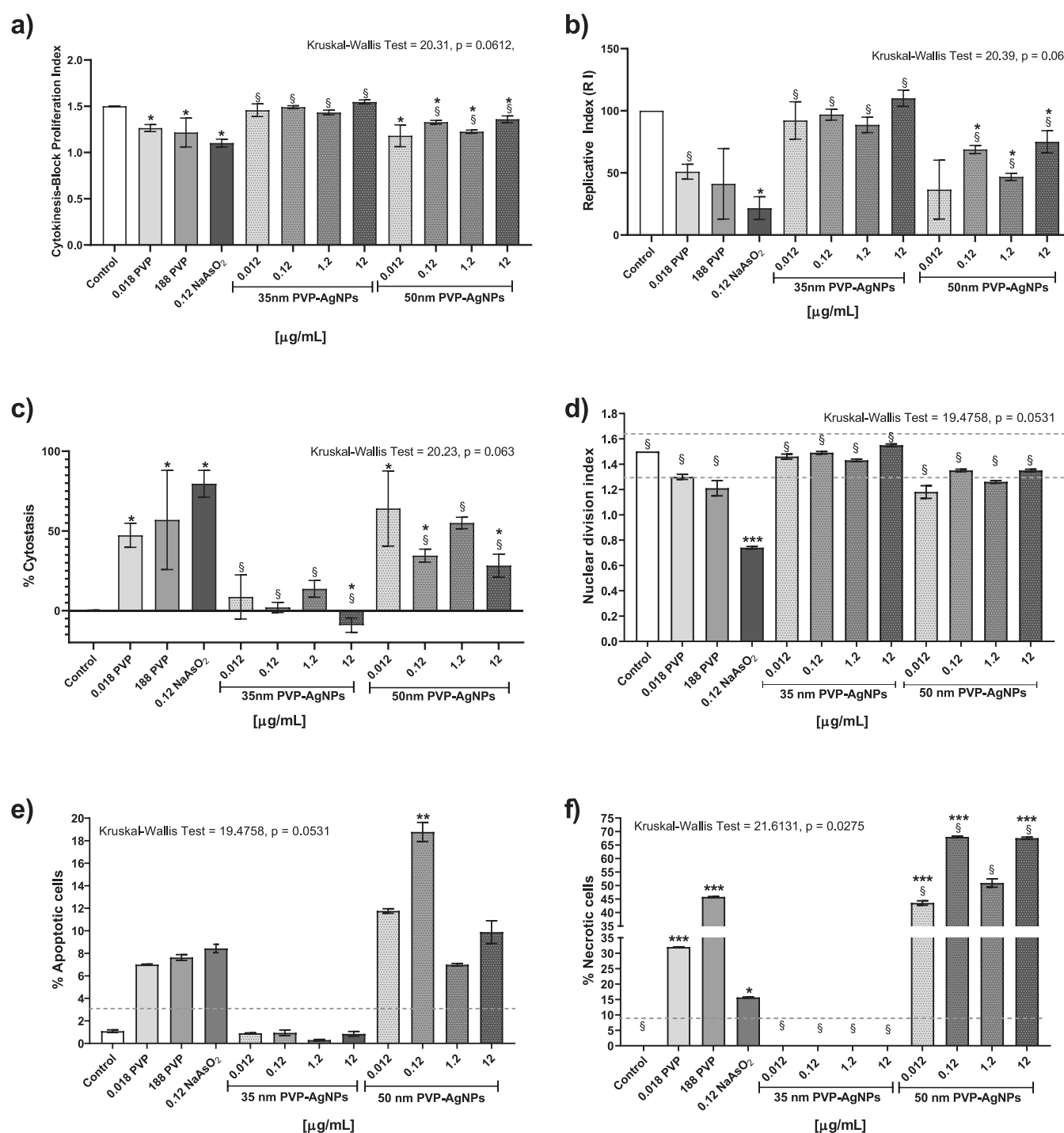


**Figure 2.** Biomarkers of cytotoxicity in human peripheral blood lymphocytes (HPBLs) cultured in vitro with 35 and 50 nm PVP-AgNPs at different concentrations: 0.012, 0.12, 1.2, and 12  $\mu\text{g}/\text{mL}$ ; negative control, PVP control (0.0188 and 188  $\mu\text{g}/\text{mL}$ ); and positive control, NaAsO<sub>2</sub> (0.12  $\mu\text{g}/\text{mL}$ ). (a) Cytokinesis-block proliferation index (CBPI), (b) replication index (RI), (c) cytostasis percentage, (d) nuclear division index (NDI), (e) apoptosis percentage, and (f) necrosis percentage. The dotted lines show the standard values found in healthy donors for each biomarker. The nonparametric analysis of Kruskal–Wallis (the  $p$ -value is indicated on the top of each figure) was performed; the bars represent the mean  $\pm$  standard deviation of three independent experiments. \* Indicates significant differences ( $p \leq 0.05$ ), \*\* indicates very significant differences ( $p \leq 0.01$ ), and \*\*\* indicates highly significant differences ( $p \leq 0.001$ ) compared with the negative control (lymphocytes without treatment), while § indicates significant differences ( $p \leq 0.05$ ) compared with the positive control (sodium arsenite).

PVP-AgNPs produce 28.2–64.3% cytostasis at all of the concentrations evaluated, while 30 nm PVP-AgNPs do not induce cytostasis; in contrast, they seem to promote cell division with the highest concentration used (12  $\mu\text{g}/\text{mL}$ ), as shown in Figure 2c.

While CBPIs show significant differences in the cytotoxic response of the agents, a completely different result is found for the nuclear division index (NDI), where only sodium arsenite showed a difference in comparison with the control group (Figure 2d).

On the basis of apoptosis and necrosis data, we confirm the differences regarding cytotoxicity elicited by both AgNP formulations. While 35 nm PVP–AgNPs do not show differences from the control at any of the concentrations assessed, all of the concentrations of 50 nm PVP–AgNPs showed higher apoptosis induction than those of the control and even sodium arsenite (Figure 2e), although the concentration of 0.12  $\mu\text{g}/\text{mL}$  of 50 nm PVP–AgNPs was the only one that showed a statistically significant difference. Apoptosis on lymphocytes exposed to sodium arsenite increased to 8.4%, while those exposed to PVP at concentrations of 0.018 and 188  $\mu\text{g}/\text{mL}$  showed 7.0 and 7.6%, respectively. Even though none of them present a significant difference in the apoptosis induction compared with the control, the average rate of apoptotic cells found in healthy donors is 1%.<sup>17</sup> Under our experimental conditions, the apoptosis was 1.09% (Figure 2e).

On the other hand, the necrosis induction showed impressive and opposite results for 35 and 50 nm PVP–AgNPs. The 50 nm PVP–AgNPs are the most cytotoxic agents evaluated in this work, producing, at all concentrations assessed, from 43.5 to 68.0% necrotic cells, which is more than double the rate of necrosis produced by sodium arsenite. In contrast, none of the 35 nm PVP–AgNP concentrations assayed showed a significant difference compared with the control, despite the fact that the coating agent alone induced an increase of necrosis by itself (Figure 2f). The vehicle control (PVP 12.6  $\pm$  2.7 kDa) at both concentrations assessed showed induction of necrosis of 32.0 and 45.7% for the concentrations of 0.0188 and 188  $\mu\text{g}/\text{mL}$ , respectively. The necrosis found for PVP was even higher than that produced by sodium arsenite (Figure 2f). Necrosis observed in the lymphocytes exposed to sodium arsenite was 15.6  $\pm$  0.17%, almost double the upper bound of 9% reported by Fenech in healthy donors.<sup>17</sup> Under our conditions, no necrosis was identified for untreated lymphocytes (Figure 2f).

Cytotoxic results are consistent with the registered genotoxicity. Even though micronuclei frequency differences compared with the control were observed for none of the substances at any of the concentrations assessed, the nuclear damage was manifested as NBUDs and NPBs. All compounds, regardless of the concentration used, showed a micronuclei frequency within the established range for healthy donors,<sup>17</sup> marked as dotted lines in Figure 3a.

Sodium arsenite and PVP do not produce an increase in micronuclei frequency compared with the negative control but significantly increase the rate of NBUDs and NPBs (Figure 3). Micronuclei absence could be related to the high cytotoxicity, probably because nuclear damage increases as the cytotoxic damage increases. Sodium arsenite that presents the most significant decrease in RI or NDI (Figure 2) showed one of the highest frequencies registered of NBUDs and NPBs of 21.87  $\pm$  0.79 and 83.42  $\pm$  0.76 for every 1000 BN cells, respectively, only exceeded by the effect produced by the 50 nm PVP–AgNPs, whose behavior will be discussed later (Figure 3b,c).

PVP that also induces apoptosis and necrosis greater than that of the control at both concentrations assayed showed frequencies of NBUDs and NPBs of 11.06–14.74 and 27.50–36.96, respectively.

Similar results to those described for sodium arsenite and PVP were found for 50 nm PVP–AgNPs. These nanoparticles produce the highest cytotoxic and genotoxic damage among all of the compounds evaluated (Figures 2 and 3). The highest

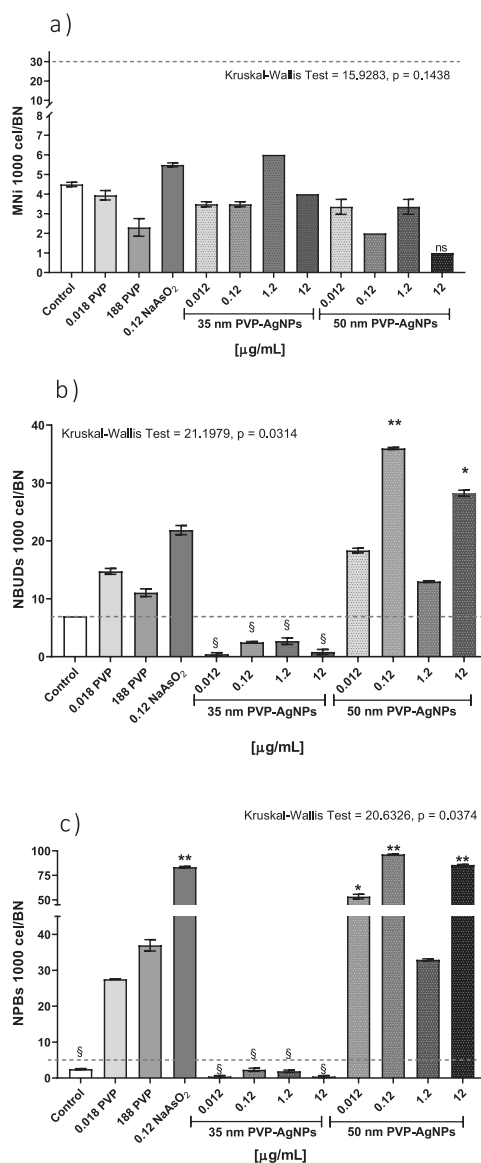


**Figure 3.** Genotoxicity biomarkers in human lymphocytes cultured in vitro with 35 and 50 nm PVP–AgNPs at different concentrations: 0.012, 0.12, 1.2, and 12  $\mu\text{g}/\text{mL}$ ; a negative control (culture without treatment); PVP control (stabilizer of 35 nm PVP–AgNPs) at 0.0188 and 188  $\mu\text{g}/\text{mL}$ ; and a positive control (0.12  $\mu\text{g}/\text{mL}$  NaAsO<sub>2</sub>). The columns represent the frequency of (a) micronuclei (MNi), (b) nuclear buds (NBUDs), and (c) nuclear bridges (NPBs) for every 1000 binucleated (BN) cells. The mean  $\pm$  standard deviation of three independent experiments are shown. The dotted line represents the average values of genotoxicity biomarkers found in healthy donors. \* Indicates significant differences ( $p \leq 0.05$ ) and \*\* indicates very significant differences ( $p \leq 0.001$ ) compared with the negative control (lymphocytes without treatment), while \$ indicates significant differences ( $p \leq 0.05$ ) compared with the positive control (sodium arsenite). The nonparametric analysis of Kruskal–Wallis (the  $p$ -value is indicated on the top of each graph) was performed.

values of apoptosis and necrosis were produced by this AgNP formulation (Figure 2). In the same way, NBUDs and NPBs showed the highest frequencies with 13–36 NBUDs and 33–96 NPBs for every 1000 BN cells (Figure 3).

In contrast, the 35 nm PVP–AgNPs produce neither cytotoxic nor genotoxic effects. None of the concentrations assessed provide statistically significant differences for any of

the nine biomarkers compared with the control (Figures 2 and 3).

## DISCUSSION

**CBMN Assay Impact.** The evaluation of cytotoxic and genotoxic effects of nanomaterials represents a contemporary issue due to their widespread presence around the world, especially for silver nanoparticles with potential biomedical applications. Furthermore, the model used for evaluating the toxicity of AgNPs remains one of the greatest challenges. In this regard, the use of reliable and comparable data from reproducible and accurate methodologies is essential to facilitate decision-making on safe work with nanomaterials. Particularly, the CBMN assay is a robust technique that allows the evaluation of the nine biomarkers simultaneously, providing remarkable results with primary cultures, especially with human peripheral blood lymphocytes (HPBLs), which, for a long time, have been identified as extremely sensitive indicators of genotoxic damage.<sup>45</sup> However, to our knowledge, this technique has been underused for the cytotoxicity and genotoxicity evaluation of AgNPs.<sup>26,46–49</sup> The results presented in Figures 2 and 3 demonstrate that the CBMN assay is a useful and reproducible technique as a first approach to determine the cytotoxic and genotoxic effects of silver nanoparticles but also show the mandatory need to consider all nine biomarkers provided by the model to establish them.

It is very important to note that NDI values for all agents assessed are within the range reported by Fenech for a population of healthy donors, 1.3–2.2,<sup>17</sup> with the exception of sodium arsenite, which shows a decrease in value to 0.7. Therefore, just analyzing NDI values could lead to the erroneous conclusion that both AgNP formulations present the same response of no cytotoxic damage.

When searching the literature for the response of other AgNP formulations regarding the evaluation of CBPI, RI, or cytostasis parameters, we could not find other studies. Even though the data are the same, the way in which multinucleated cell contribution is considered allows us to observe differences between the values of CBPI and NDI (eqs 1 and 4), although the values of the biomarkers, index of replication and percentage of cytostasis, enable us to better differentiate the cytotoxic effects of the different agents evaluated.

Furthermore, none of the reference substances recommended by the OECD on Guideline 487 “In Vitro Mammalian Cell Micronucleus Test”<sup>15</sup> produce cytotoxic and genotoxic damage through ROS overproduction; instead, they produce cell damage by direct interaction with DNA, inhibiting DNA synthesis, or interacting with the microtubules and interfering with their functions.

**Arsenic Cytotoxic Effect on HPBLs.** The arsenic cytotoxic and genotoxic effects on HPBLs have been widely described in the literature.<sup>50,51</sup> Half-inhibitory concentration (IC<sub>50</sub>) of sodium arsenite on peripheral mononuclear (MONO) cells has been reported as time-dependent, with values higher than 10  $\mu\text{M}$  (1.29  $\mu\text{g}/\text{mL}$ ) after 24 h of exposure and 5  $\mu\text{M}$  (0.64  $\mu\text{g}/\text{mL}$ ) after 48 and 72 h.<sup>52</sup> Cytotoxicity of sodium arsenite could be triggered by reactive nitrogen species (RNS) and reactive oxygen species (ROS) in a mitochondrial-dependent pathway, which could overwhelm the antioxidant system of the cells eliciting the apoptotic and necrotic processes.<sup>51,53</sup>

Due to the lack of data related to CBPI, RI, or percentage of cytostasis for sodium arsenite in human lymphocytes, we use

the NDI values for comparative purposes. The NDI value found in the present work for HPBL exposure to 1  $\mu\text{M}$  sodium arsenite agrees with that reported by Colognato<sup>54</sup> (Figure 2).

The production of ROS could explain the increase of apoptosis and necrosis events promoted by sodium arsenite on HPBLs found in this work (Figure 2e,f). Apoptosis is 2 times higher than that registered for the control, while necrosis is 4 times higher. It is important to recall that lymphocytes were exposed only for 20 h to sodium arsenite due to its high toxicity. This fact also explains the lack of differences found in the micronuclei frequency compared with the control.

However, this does not mean that nuclear damage promoted by sodium arsenite does not exist. We could not expose the arsenite at the same time as AgNPs because it leads to complete lymphocyte decomposition. Measurement of only the micronucleus for genotoxicity evaluation is not enough; frequencies of nuclear buds and nucleoplasmic bridges (NPBs) should also be measured.

We observed nuclear damage by the substantial increase of BUDs and especially of PBDs. MNi can originate from fragmented chromosome material when NPBs are formed, stretched, and broken during telophase. NPBs arising from misrepair of DNA breaks are also likely to be associated with MNi originating from the acentric fragment generated during misrepair. Therefore, the presence of NPBs but no MNi could be related to the repair capacity of the cell within a specific time frame.<sup>18</sup> A similar effect to that described for sodium arsenite was found with hydrogen peroxide.<sup>16</sup>

**Cytotoxic and Genotoxic Effects of PVP.** Contrary to sodium arsenite, scarce information about the cytotoxic effects of PVP directly on HPBLs can be found. The lack of information could be due to the extremely low toxicity generally reported for this polymer. The half-lethal dose (LD<sub>50</sub>) commonly reported for PVP is higher than 100 g/kg administered orally and 10 g/kg intravenously or intraperitoneally.<sup>55</sup> Unfortunately, in many of the reports, the molecular weight of the employed polymer is not indicated,<sup>56</sup> although PVP toxicity relies upon it.<sup>57</sup> Just analyzing the NDI values, it seems reasonable that PVP, at both concentrations employed here, does not affect cell division of HPBLs exposed to it (Figure 2a). However, both PVP concentrations assayed present similar CBPI, RI, cytostasis, and apoptosis and even a higher necrosis induction than that of sodium arsenite (Figure 2b,c). Thus, PVP used in this work (with a molecular weight of 12.6  $\pm$  2.7 kDa) is not entirely innocuous as claimed in the literature, at least for the isolated HPBL cultures. The obtained result is a clear example that NDI does not provide enough information about the cytotoxicity of the substances.

Surprisingly for us, the same can be said for the genotoxicity elicited by PVP recorded as the MNi frequency. Although the micronuclei frequency is less than the value found in healthy donors, the rate of NBUDs and NPBs is always higher than the reference value and, for both concentrations of PVP assessed, those biomarkers are several times higher than the values found for the control (Figure 3).

**AgNPs Cytotoxicity and Genotoxicity.** Now, for different AgNP formulations, no changes in NDI and MNi compared with the negative control were observed (Figure 2). However, analyzing the data for CBPI, RI, cytostasis, apoptosis, necrosis, NBUDs, and NPBs, a different trend was found. While 35 nm PVP–AgNPs produce no changes in CBPI, RI, cytostasis, apoptosis, or necrosis compared with the control, 50 nm PVP–AgNPs produce the highest amount of

apoptosis, necrosis, NBUDs, and NPBs of all assayed compounds, producing almost the same frequency of NPBs and twice the necrosis and NBUDs than that induced by sodium arsenite.

As previously reported,<sup>18</sup> NBUDs can be interpreted as DNA-damage repair attempts by amplifying the genetic material that is removed during the S phase of the cell cycle.<sup>58,59</sup> On the other hand, the NPBs originate during anaphase and are formed when the centromeres of the dicentric chromosomes extend to the opposite poles of the cell during mitosis, resulting in a union between both new nuclei formed.<sup>18,60,61</sup>

**Reasons for Differences in Cyto- and Genotoxicity of Two Types of AgNPs.** Despite the similarity in the size, shape,  $\zeta$  potential, and coating of 35 and 50 nm PVP–AgNPs, we found enormous differences in the response of human peripheral blood lymphocytes to these nanoparticles. These results reflect nucleic material damage that could be caused by the formation of amplified telomeric regions of DNA that can eventually be separated from the nucleus, creating chromosomal aberrations such as NBUDs and NPBs, which ultimately could be manifested as MNi.<sup>18,61</sup>

Furthermore, the above results are opposite to the findings described in other studies, where the smaller the AgNPs, the greater the cytotoxic and genotoxic damage;<sup>24,26–28</sup> thus, other factors must contribute to the differential response observed.

Several studies describe that the use of PVP as a coating agent decreases the cytotoxic and genotoxic effects of AgNPs for different cell types compared with bare nanoparticles or other coating agents such as citrate.<sup>62</sup> Vecchio and co-workers found that PVP–AgNPs decrease the genotoxic damage on human lymphocytes compared with citrate–AgNPs despite the size. Even for the smaller nanoparticles, the genotoxic effects were milder when PVP was used as a coating agent compared with AgNPs of similar size stabilized with citrate.<sup>26</sup> Even then, the changes found by Vecchio and co-workers are not as remarkable as those found in this work, but we must consider that they only analyzed the difference in the frequency of micronuclei without consideration of any other biomarker.

**Contribution of Silver Ion Toxicity.** The most important changes regarding cytotoxicity and genotoxicity could be expected for less stable AgNPs if we consider that  $IC_{50}$  for silver ions on HPBLs is 1.1  $\mu\text{M}$  (0.1  $\mu\text{g}/\text{mL}$   $\text{Ag}^+$ ). Several reports have shown that these less stable AgNP formulations, such as uncoated 3–7 nm AgNPs studied by Joksić and co-workers,<sup>24</sup> produced a significant increase of cytotoxic and genotoxic damage with size and concentration dependencies on human lymphocytes. Despite the fact that the higher the nanoparticle concentration, the lower the NDI and the higher the MNi frequency,<sup>24</sup> no generalization in the biological response can be made because, in the same work, the authors found that 2 nm uncoated AgNPs promote cell proliferation, which is closely related to a definite increase of insulin-like growth factor-1.<sup>24</sup>

A further interesting example of the coating agent effect on human lymphocytes is provided by Ivask and co-workers, who found that citrate–AgNPs ( $IC_{50} = 12.5 \mu\text{g}/\text{mL}$ ) are less cytotoxic than the more stable polyethyleneimine–AgNPs ( $IC_{50} = 5.25 \mu\text{g}/\text{mL}$ ), both nanoparticles with practically the same size (18 nm).<sup>27</sup> The cytotoxicity of the former is attributed to the  $\text{Ag}^+$  ion release due to its lower stability, while for the latter, the cytotoxicity is attributed to the whole nanoparticle. The dissolution rate shows that the released ions

by polyethyleneimine–AgNPs cannot generate the cytotoxic damage observed. Interestingly, both 18 nm AgNPs promote the appearance of apoptosis markers in 10% of the cells at all evaluated concentrations, while a concentration-dependent behavior was observed for necrosis, reaching values up to 50% of the cell population for the higher concentrations employed.<sup>27</sup>

In the present work, a fairly comparable response on the necrosis induction was found on lymphocytes exposed to 50 nm PVP–AgNPs, reaching up to 45%, but just the opposite response for 35 nm PVP–AgNPs. This allows us to propose that silver ion release from 35 nm PVP–AgNPs could not be much faster than, or in comparable amounts to, silver ions released by 50 nm PVP–AgNPs.

**Ag/PVP Ratio Impact on Toxicity.** To our knowledge, despite the differences in the size and coating agents employed, none of the revised results have shown sharp differences in cytotoxicity and genotoxicity such as those found here. We consider that the differences of HPBL responses could rely upon the Ag/PVP ratio used to fabricate these PVP–AgNP formulations. According to the corresponding suppliers, Ag/PVP w/w ratios for 35 and 50 nm PVP–AgNP formulations are 6/94 and 36/64, respectively. The small concentration of Ag and the high concentration of the PVP stabilizer in the 35 nm PVP–AgNP formulation prevent the release of an essential amount of silver ions that could produce cytotoxic and genotoxic damage. Our research group has determined that after 24 h of incubation in Roswell Park Memorial Institute (RPMI) medium, the silver ion released from 10  $\mu\text{g}/\text{mL}$  solution of 35 nm PVP–AgNP formulation was 0.024  $\mu\text{g}/\text{mL}$ , quantified by inductively coupled plasma optical emission spectrometry (ICP-OES),<sup>63</sup> which is 1000-fold lower than the dietary silver intake in Canadian women (27  $\mu\text{g}/\text{day}$ ), and at least 16-fold the human use level for the general population (0.4–30  $\mu\text{g}/\text{day}$ ).<sup>64</sup> Therefore, the biological response observed for this formulation cannot be attributable even to the silver ion released or to the coating agent.

Despite the fact that the coating agent elicits its own cytotoxic and genotoxic damage, the response is still different from that observed for the whole nanoparticle. The results suggest that the lack of cytotoxic response for 35 nm PVP–AgNPs can be attributable to the whole nanoparticle, which has a very stable formulation achieved by the high amount of PVP employed. In contrast, the use of a lower amount of coating agent could produce a less stable formulation, from which the released silver ions increase the cytotoxic and genotoxic damage like that observed for 50 nm PVP–AgNPs.

The higher stability due to the significant amount of PVP in the 35 nm PVP–AgNP formulation also could help explain the remarkable antitumor activity of this formulation observed in mice with melanoma, which decreases more than twice the tumor growth compared with cisplatin, but without apparent genotoxic damage observed for the mice.<sup>41</sup>

**Impact of the Cellular Type Exposed to AgNPs.** The identification of the factors that provoke the biological response of each formulation of AgNPs is critical. The differential cytotoxicity elicited by AgNPs is related not only to their physicochemical characteristics but also to the cellular type to which they are exposed. Greulich and co-workers<sup>30</sup> show that concentrations of 30  $\mu\text{g}/\text{mL}$  (regarding total silver) of specific PVP–AgNP formulations do not decrease the cellular viability of T-lymphocytes isolated from human peripheral blood, while concentrations starting from 20  $\mu\text{g}/$

mL of the same PVP–AgNPs show a concentration-dependent behavior in monocyte viability of the same blood sample. A commercially available 20–30 nm PVP–AgNP formulation also presents differential toxicity between tumorigenic and nontumorigenic cells (PVP, 0.2 wt % SkySpring Nanomaterials, Inc., Houston, TX). This formulation showed higher growth inhibition potency on triple-negative breast cancer cells MDA-MB-231, BT-549, and SUM-159 than those in the nontumorigenic cell lines MCF-10A, human mammary epithelial cells (HMECs) (184B5), and in post-stasis HMECs.<sup>65</sup>

**Concentrations of 35 nm PVP–AgNPs Effective as Antiproliferative, Antitumor, and Antiviral Agents.** Comparing the results obtained in this work with others found by our group about the viability of human tumor cell lines exposed to the same 35 nm PVP–AgNP formulation, we found an excellent selectivity regarding cytotoxic effects. We found that  $IC_{50}$  values for 35 nm PVP–AgNPs on breast (MDA-MB-231 and MCF-7), cervix (HeLa), prostate (DU-145), colorectal (DLD-1 and HT-29), and lung (H1299 and H1437) human tumor cell lines are within the range 1.82–3.43  $\mu\text{g}/\text{mL}$  after 24 h of exposure. In all of the tumor cells, apoptosis is the main activated pathway, probably triggered by ROS overproduction. No evidence of DNA damage or genotoxicity was observed on these cells.<sup>31</sup> It is remarkable that a concentration of 12  $\mu\text{g}/\text{mL}$  that represents 3.5–6.6 times higher concentration than that used to eliminate the half-population of tumor cell cultures does not show any sign of cytotoxicity and much less of genotoxicity on human peripheral blood lymphocytes (Figures 2 and 3). The above-described selective cytotoxic effect provides an opportunity to continue the AgNP preclinical protocols for cancer treatment.

Other uses of this AgNP formulation, by which humans can be in touch with it, include its use as an antiviral agent against the white spot syndrome virus (WSSV),<sup>42</sup> treatment of canine distemper,<sup>37</sup> or application as sanitizing and hormetic agents on plant micropropagation cultures.<sup>39,40</sup>

As far as we know, this is the first report on the effect of silver nanoparticle formulations using the nine biomarkers provided by the blocking cytokinesis (CBMN) assay in human lymphocyte cells from healthy donors. Furthermore, this is the first time that enormous differences regarding the cytotoxic and genotoxic effects of AgNP formulations that are quite similar in size, shape,  $\zeta$  potential, and coating agent were reported.

## CONCLUSIONS

This work allows us to conclude that the CBMN assay using human blood peripheral lymphocytes with the analysis of the nine biomarkers provided by the technique is a useful, reproducible, and low-cost option as a first approach to the cytotoxicity and genotoxicity of nanomaterials.

The 35 nm PVP–AgNP formulation (Argovit) presents no evidence of cytotoxic or genotoxic damage to the human peripheral blood lymphocytes for the studied concentrations, in contrast to the very similar AgNP formulation (50 nm PVP–AgNPs, NanoComposix). Due to this comparison, the fundamental role played by the [coating agent]/[metal] ratio in the biological response of the manufactured nanoparticles and their toxicity was suggested, providing valuable information for the design and production of safe nanomaterials.

The use of the nine biomarkers instead of the two or three commonly reported in the literature provides impressive

differences with respect to the cytotoxic and genotoxic potential of the nanomaterials evaluated. As was shown in this work, this technique is a very sensitive and powerful tool that allows researchers to establish the cytotoxic and genotoxic differences of two AgNP formulations with very similar physicochemical properties and that did not seem harmful when evaluating the common biomarkers' nuclear division index and the frequency of micronuclei.

The obtained results also revealed the cytotoxic selectivity of the AgNP formulation Argovit. The concentrations used to produce remarkable growth inhibition in several systems such as tumor cells, virus, and pathogen bacteria are the same ones that produce scarce cytotoxic and genotoxic damage on primary human culture (lymphocytes). This selectivity can be applied to generate therapeutic alternatives not only for cancer, virus, or bacteria but also for immunologic, neurodegenerative, or chronic–degenerative diseases.

These results will contribute to providing a complete picture regarding the safe production and use of manufactured AgNP formulations in the different application areas already explored and the new ones to come.

## MATERIALS AND METHODS

**Silver Nanoparticles (AgNPs).** We selected the commercially available AgNP formulation Argovit because it has been used in multiple application areas and has certificates for use in veterinary and human applications.<sup>33,37</sup> Silver nanoparticles were donated by Dr. Vasily Burmistrov of the Vector-Vita Scientific and Production Center (Novosibirsk, Russia). This AgNP formulation has been previously characterized by transmission electron microscopy (TEM) and has been described to have a spheroidal shape with a diameter distribution between 1 and 90 nm, with an average size of  $35 \pm 12$  nm. The hydrodynamic diameter is 70 nm, with a  $\zeta$  potential of  $-15$  mV, and a plasmon resonance found at 420 nm. This formulation is a stable aqueous suspension that contains 1.2% weight of metallic silver stabilized with 18.8% weight of PVP ( $12.6 \pm 2.7$  kDa, Boai NKY Pharmaceuticals, China). The final concentration of Argovit is 200 mg/mL (20%) AgNPs.<sup>41</sup> From here on, this formulation is identified as 35 nm PVP–AgNPs.

Besides, we used the commercially available AgNP formulation Eonix silver nanospheres dried powder (NanoComposix, San Diego, CA) under the same experimental conditions for comparative purposes. The size of this AgNP formulation reported by the provider for this batch is  $51 \pm 9$  nm. The metallic silver content is 34% of the mass and 66% of PVP 40 kDa as the coating agent. Plasmon resonance was reported at 430 nm. The resuspension of AgNPs was carried out following the recommendations of the provider with distilled water to obtain a stock solution of 1.2 mg/mL. From here on, this formulation is identified as 50 nm PVP–AgNPs.

**Cytokinesis-Block Micronucleus (CBMN) Assay on Human Lymphocyte Cultures.** The cytokinesis-block micronucleus (CBMN) assay on human lymphocyte cultures was conducted as described by Fenech.<sup>66</sup> The first step consists of the addition of 0.5 mL of heparinized peripheral blood from a normocytic nonsmoking 38-year-old male donor to 6.3 mL of *N*-(2-hydroxyethyl)piperazine-*N'*-ethanesulfonic acid (HEPES) RPMI-1640 modified medium (Sigma R5886, St. Louis, MO) supplemented with 1% L-glutamine (Sigma G6392, St. Louis, MO), 1% of nonessential amino acids

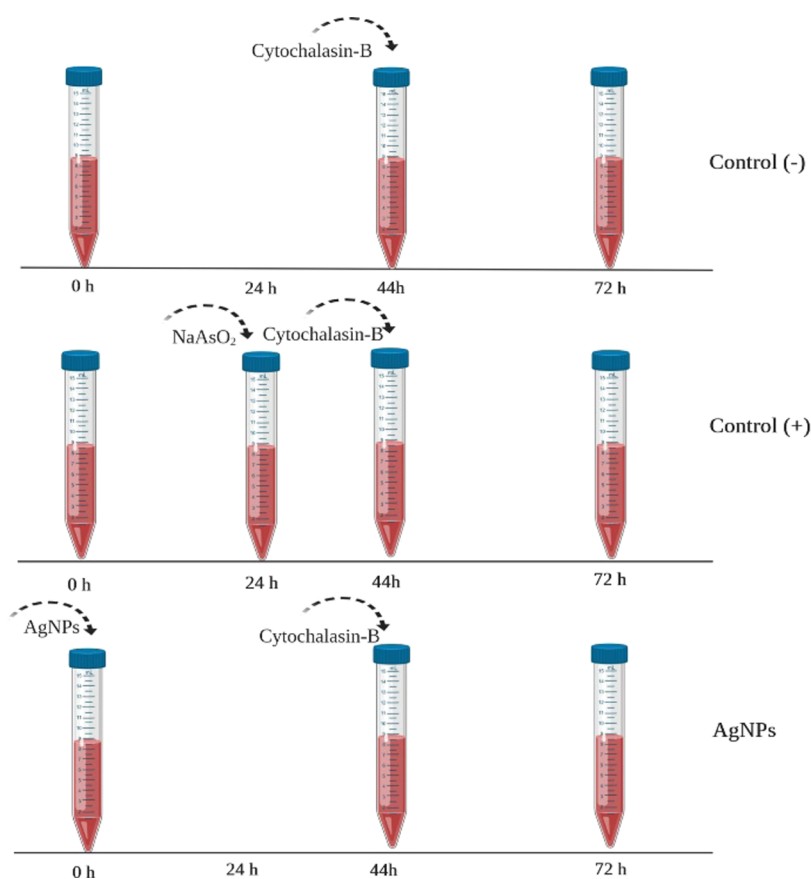


**Figure 4.** Schematic representation of the procedure. The tubes represent the blood cultures treated with AgNPs or NaAsO<sub>2</sub> as indicated.

(Sigma M7145, St. Louis, MO), and 0.2 mL of phytohemagglutinin (1 mg/mL) (Sigma L2646, St. Louis, MO)

The lymphocytes were incubated at 37 °C and exposed to different concentrations of AgNPs: 0.012, 0.12, 1.2, and 12 μg/mL. Dilutions were calculated according to the metallic silver content in the Argovit and nanoComposix formulations. Physiological solution and NaAsO<sub>2</sub> (0.12 μg/mL) (Sigma S7400, St. Louis, MO) were used as negative and positive controls of cytotoxic and genotoxic effects, respectively. In our experiment, NaAsO<sub>2</sub> was added 24 h later than the rest of the assayed compounds to avoid masking the genotoxic damage manifested as NBUDs and NPBs by its powerful cytotoxic effect. An additional experiment with PVP (0.0188 and 188 μg/mL) was included to differentiate the impact of the coating agent from that elicited by AgNPs. After 44 h of incubation, the addition of 21 μL of cytochalasin B (Sigma C6762, St. Louis, MO) at 2 mg/mL blocks cell cytokinesis (Figure 4). The cultures were incubated at 37 °C for another 28 h until harvest. After 72 h of culture, the lymphocytes were harvested through centrifugation, fixed with a methanol (Sigma-Aldrich 34860, St. Louis, MO)–acetic acid (Sigma-Aldrich ARK2183, St. Louis, MO) solution, and placed on a slide for later staining with eosin B (Sigma 2853, St. Louis, MO) and methylene blue (Sigma O3978, St. Louis, MO). Cells were counted using a light field microscope (Primo Star Zeiss) with a 100× objective lens.

The CBPI and replication index (RI) were calculated by counting 1000 cells, including mononuclear (MONO), binucleated (BN), trinucleated (TRIN), and tetranucleated (TETRAN) cells<sup>44</sup> according to eqs 1 and 2, respectively

$$CBPI = \frac{((\#MONO \text{ cells}) + (2 \times \#BN \text{ cells}) + (3 \times \#MULTIN \text{ cells}))}{(\text{total number of cells})} \quad (1)$$

where *T* is the test chemical treatment culture, *C* is the control culture, and MULTIN = trinucleated + tetranucleated cells.

$$RI = \frac{((\#BN \text{ cells}) + (2 \times \#MULTIN \text{ cells})) / (\text{total \# of cells})_T}{((\#BN \text{ cells}) + (2 \times \#MULTIN \text{ cells})) / (\text{total \# of cells})_C} \quad (2)$$

The cytostasis percentage is defined as follows

$$\% \text{ cytostasis} = 100 - 100 \times \frac{CBPI_T - 1}{CBPI_C - 1} \quad (3)$$

Also, the nuclear division index was determined for comparative purposes according to the following formula<sup>66</sup>

$$NDI = \frac{(\#MONO) + (2 \times \#BN) + (3 \times \#TRIN) + (4 \times \#TETRAN)}{(\text{total number of cells})} \quad (4)$$

The same number of cells was used to quantify apoptosis and necrosis.<sup>16</sup> Frequencies of micronuclei (MNI), nuclear out-breaks (NBUDs), and chromatin bridges (NPBs) were quantified on 1000 binucleated (BN) cells with a well-preserved cytoplasm to evaluate the genotoxic effect of each treatment.<sup>17</sup> The scheme in Figure 4 represents the procedure described above.

**Statistics.** To guarantee the homoskedasticity between the experimental groups, a square root transformation was carried out,<sup>67</sup> which is suggested for the variables with the goodness of



fit to the Poisson model, such as micronuclei and other nuclear anomalies,<sup>68</sup> according to the following formula

$$\hat{X} = \sqrt{\left(X + \frac{1}{2}\right)} \quad (5)$$

$\hat{X}$  is the estimator of the transformed variable and  $X$  is the original variable, number of counted anomalies.

The transformed data were analyzed using the StatSoft and Graph-Pad-Prism v8. A Kruskal–Wallis test was performed with Tukey's post hoc multiple comparison test. \* Indicates significant differences ( $p \leq 0.05$ ), \*\* indicates very significant differences ( $p \leq 0.01$ ), and \*\*\* indicates highly significant differences ( $p \leq 0.001$ ) compared with the negative control (lymphocytes without treatment), while § indicates significant differences ( $p \leq 0.05$ ) compared with the positive control (sodium arsenite). The  $p$ -value of each analysis is indicated on the top of the corresponding figure.

## AUTHOR INFORMATION

### Corresponding Authors

**María Evarista Arellano-García** – Laboratorio de Genotoxicología Ambiental, Facultad de Ciencias, Universidad Autónoma de Baja California, C.P. 22860 Ensenada, Baja California, México; [orcid.org/0000-0002-0997-6902](https://orcid.org/0000-0002-0997-6902); Email: [evarista.arellano@uabc.edu.mx](mailto:evarista.arellano@uabc.edu.mx)

**Yanis Toledano-Magaña** – Escuela de Ciencias de la Salud, Universidad Autónoma de Baja California, C.P. 22890 Ensenada, Baja California, México; [orcid.org/0000-0002-2595-7939](https://orcid.org/0000-0002-2595-7939); Email: [yanis.toledano@uabc.edu.mx](mailto:yanis.toledano@uabc.edu.mx)

### Authors

**Balam Ruiz-Ruiz** – Laboratorio de Genotoxicología Ambiental, Facultad de Ciencias, Universidad Autónoma de Baja California, C.P. 22860 Ensenada, Baja California, México

**Patricia Radilla-Chávez** – Escuela de Ciencias de la Salud, Universidad Autónoma de Baja California, C.P. 22890 Ensenada, Baja California, México

**David Sergio Salas-Vargas** – Escuela de Ciencias de la Salud, Universidad Autónoma de Baja California, C.P. 22890 Ensenada, Baja California, México

**Francisco Casillas-Figueroa** – Escuela de Ciencias de la Salud, Universidad Autónoma de Baja California, C.P. 22890 Ensenada, Baja California, México

**Roberto Luna Vazquez-Gomez** – Escuela de Ciencias de la Salud, Universidad Autónoma de Baja California, C.P. 22890 Ensenada, Baja California, México

**Alexey Pstryakov** – Department of Technology of Organic Substances and Polymer Materials, Tomsk Polytechnic University, 634050 Tomsk, Russia

**Juan Carlos García-Ramos** – Escuela de Ciencias de la Salud, Universidad Autónoma de Baja California, C.P. 22890 Ensenada, Baja California, México

**Nina Bogdanchikova** – Centro de Nanociencias y Nanotecnología, Universidad Nacional Autónoma de México, C.P. 22879 Ensenada, Baja California, México

Complete contact information is available at:

<https://pubs.acs.org/10.1021/acsoomega.0c00149>

### Author Contributions

The manuscript was written through the contributions of all authors. All authors have given approval to the final version of the manuscript.

### Funding

This work was supported by Conacyt 293418 (Red Internacional de Bionanotecnología con Impacto en Bio-medicina, Alimentación y Bioseguridad) and Tomsk Polytechnic University Competitiveness Enhancement Program, project VIU-ISHBMT-65/2019.

### Notes

The authors declare no competing financial interest.

## ACKNOWLEDGMENTS

The authors thank Conacyt for the scholarship 227890/208648 and Project 294727 (Farmoquímicos) for the specialist network provided.

## ABBREVIATIONS

AgNPs, silver nanoparticles; PVP, poly(vinylpyrrolidone); PVP–AgNPs, poly(vinylpyrrolidone)-coated silver nanoparticles; NDI, nuclear division index; MI, mitotic index; MNi, micronuclei; % Cyt, cytostasis percentage; NBUDs, nuclear buds; NPBs, nucleoplasmic bridges; CBMN, cytokinesis-block micronucleus; MONO, mononuclear; BN, binucleated; TRIN, trinucleated; TETRAN, tetranucleated; ROS, reactive oxygen species; RNS, reactive nitrogen species; CMC, carboxymethylcellulose; WSSV, white spot syndrome virus; HPBL, human peripheral blood lymphocyte; IC<sub>50</sub>, half-inhibitory concentration; LD<sub>50</sub>, half-lethal dose

## REFERENCES

- (1) Chmielowiec-Korzeniowska, A.; Krzosek, L.; Tymczyna, L.; Pyrz, M.; Drabik, A. Bactericidal, Fungicidal and Virucidal Properties of Nanosilver. Mode of Action and Potential Application. A Review. *Ann. Univ. Mariae Curie-Sklodowska, Sect. EE* **2013**, *31*, 1–11.
- (2) Pulit, J.; Banach, M.; Kowalski, Z. Nanosilver - Making Difficult Decisions. *Ecol. Chem. Eng.* **2011**, *18*, 185–196.
- (3) Burduşel, A.-C.; Gherasim, O.; Grumezescu, A. M.; Mogoantă, L.; Fica, A.; Andronescu, E. Biomedical Applications of Silver Nanoparticles: An Up-to-Date Overview. *Nanomaterials* **2018**, *8*, No. 681.
- (4) Liao, C.; Li, Y.; Tjong, S. C. Bactericidal and Cytotoxic Properties of Silver Nanoparticles. *Int. J. Mol. Sci.* **2019**, *20*, No. 449.
- (5) Foldbjerg, R.; Jiang, X.; Micleuş, T.; Chen, C.; Autrup, H.; Beer, C. Silver Nanoparticles - Wolves in Sheep's Clothing? *Toxicol. Res.* **2015**, *4*, 563–575.
- (6) Kermanizadeh, A.; Cauché, C.; Brown, D. M.; Loft, S.; Moller, P. The Role of Intracellular Redox Imbalance in Nanomaterial Induced Cellular Damage and Genotoxicity: A Review. *Environ. Mol. Mutagen.* **2015**, *56*, 111–124.
- (7) Kędziora, A.; Speruda, M.; Krzyżewska, E.; Rybka, J.; Łukowiak, A.; Bugła-Płoskońska, G. Similarities and Differences between Silver Ions and Silver in Nanoforms as Antibacterial Agents. *Int. J. Mol. Sci.* **2018**, *19*, No. 444.
- (8) García-Reyero, N.; Kennedy, A. J.; Escalon, B. L.; Habib, T.; Laird, J. G.; Rawat, A.; Wiseman, S.; Hecker, M.; Denslow, N.; Stevens, J. A.; et al. Differential Effects and Potential Adverse Outcomes of Ionic Silver and Silver Nanoparticles in Vivo and in Vitro. *Environ. Sci. Technol.* **2014**, *48*, 4546–4555.
- (9) Li, Y.; Qin, T.; Ingle, T.; Yan, J.; He, W.; Yin, J. J.; Chen, T. Differential Genotoxicity Mechanisms of Silver Nanoparticles and Silver Ions. *Arch. Toxicol.* **2017**, *91*, 509–519.
- (10) Brkić Ahmed, L.; Milić, M.; Pongrac, I. M.; Marjanović, A. M.; Mlinarić, H.; Pavičić, I.; Gajović, S.; Vinković Vrček, I. Impact of Surface Functionalization on the Uptake Mechanism and Toxicity Effects of Silver Nanoparticles in HepG2 Cells. *Food Chem. Toxicol.* **2017**, *107*, 349–361.

- (11) Demir, E.; Vales, G.; Kaya, B.; Creus, A.; Marcos, R. Genotoxic Analysis of Silver Nanoparticles in *Drosophila*. *Nanotoxicology* **2011**, *5*, 417–424.
- (12) Bondarenko, O.; Juganson, K.; Ivask, A.; Kasemets, K.; Mortimer, M.; Kahru, A. Toxicity of Ag, CuO and ZnO Nanoparticles to Selected Environmentally Relevant Test Organisms and Mammalian Cells in Vitro: A Critical Review. *Arch. Toxicol.* **2013**, *87*, 1181–1200.
- (13) Patlolla, A. K.; Hackett, D.; Tchounwou, P. B. Genotoxicity Study of Silver Nanoparticles in Bone Marrow Cells of Sprague–Dawley Rats. *Food Chem. Toxicol.* **2015**, *85*, 52–60.
- (14) Elespuru, R.; Pfuhrer, S.; Aardema, M. J.; Chen, T.; Doak, S. H.; Doherty, A.; Farabaugh, C. S.; Kenny, J.; Manjanatha, M.; Mahadevan, B.; et al. Genotoxicity Assessment of Nanomaterials: Recommendations on Best Practices, Assays, and Methods. *Toxicol. Sci.* **2018**, *164*, 391–416.
- (15) OECD. *Guideline for the Testing of Chemicals: In Vitro Mammalian Cell Micronucleus Test*, Test No. 487; OECD, 2016.
- (16) Fenech, M.; Crott, J.; Turner, J.; Brown, S. Necrosis, Apoptosis, Cytostasis and DNA Damage in Human Lymphocytes Measured Simultaneously within the Cytokinesis-Block Micronucleus Assay: Description of the Method and Results for Hydrogen Peroxide. *Mutagenesis* **1999**, *14*, 605–612.
- (17) Fenech, M. Cytokinesis Block Micronucleus Cytome Assay. *Nat. Protoc.* **2007**, *2*, 1084–1104.
- (18) Fenech, M.; Kirsch-Volders, M.; Natarajan, A. T.; Surrallés, J.; Crott, J. W.; Parry, J.; Norppa, H.; Eastmond, D. A.; Tucker, J. D.; Thomas, P. Molecular Mechanisms of Micronucleus, Nucleoplasmic Bridge and Nuclear Bud Formation in Mammalian and Human Cells. *Mutagenesis* **2011**, *26*, 125–132.
- (19) Fenech, M.; Knasmueller, S.; Bolognesi, C.; Bonassi, S.; Holland, N.; Migliore, L.; Palitti, F.; Natarajan, A. T.; Kirsch-Volders, M. Molecular Mechanisms by Which in Vivo Exposure to Exogenous Chemical Genotoxic Agents Can Lead to Micronucleus Formation in Lymphocytes in Vivo and Ex Vivo in Humans. *Mutat. Res., Rev. Mutat. Res.* **2016**, *12*–25.
- (20) Sahu, S. C.; Roy, S.; Zheng, J.; Yourick, J. J.; Sprando, R. L. Comparative Genotoxicity of Nanosilver in Human Liver HepG2 and Colon Caco2 Cells Evaluated by Fluorescent Microscopy of Cytochalasin B-Blocked Micronucleus Formation. *J. Appl. Toxicol.* **2014**, *34*, 1200–1208.
- (21) Ghosh, M.; J, M.; Sinha, S.; Chakraborty, A.; Mallick, S. K.; Bandyopadhyay, M.; Mukherjee, A. In Vitro and in Vivo Genotoxicity of Silver Nanoparticles. *Mutat. Res., Genet. Toxicol. Environ. Mutagen.* **2012**, *749*, 60–69.
- (22) Yan, J.; Zhou, T.; Cunningham, C. K.; Chen, T.; Jones, M. Y.; Abbas, M.; Li, Y.; Mei, N.; Guo, X.; Moore, M. M.; et al. Size- and Coating-Dependent Cytotoxicity and Genotoxicity of Silver Nanoparticles Evaluated Using in Vitro Standard Assays. *Nanotoxicology* **2016**, *10*, 1373–1384.
- (23) Bandyopadhyay, A.; Banerjee, P. P.; Shaw, P.; Mondal, M. K.; Das, V. K.; Chowdhury, P.; Karak, N.; Bhattacharya, S.; Chattopadhyay, A. Cytotoxic and Mutagenic Effects of Thuja Occidentalis Mediated Silver Nanoparticles on Human Peripheral Blood Lymphocytes. *Mater. Focus* **2017**, *6*, 290–296.
- (24) Joksić, G.; Stašić, J.; Filipović, J.; Šobot, A. V.; Trtica, M. Size of Silver Nanoparticles Determines Proliferation Ability of Human Circulating Lymphocytes in Vitro. *Toxicol. Lett.* **2016**, *247*, 29–34.
- (25) Vijaya, P. P.; Rekha, B.; Mathew, A. T.; Ali, M. S.; Yogananth, N.; Anuradha, V.; Parveen, P. K. Antigenotoxic Effect of Green-Synthesised Silver Nanoparticles from *Ocimum sanctum* Leaf Extract against Cyclophosphamide Induced Genotoxicity in Human Lymphocytes-in Vitro. *Appl. Nanosci.* **2014**, *4*, 415–420.
- (26) Vecchio, G.; Fenech, M.; Pompa, P. P.; Voelcker, N. H. Lab-on-a-Chip-Based High-Throughput Screening of the Genotoxicity of Engineered Nanomaterials. *Small* **2014**, *10*, 2721–2734.
- (27) Ivask, A.; Voelcker, N. H.; Seabrook, S. A.; Hor, M.; Kirby, J. K.; Fenech, M.; Davis, T. P.; Ke, P. C. DNA Melting and Genotoxicity Induced by Silver Nanoparticles and Graphene. *Chem. Res. Toxicol.* **2015**, *28*, 1023–1035.
- (28) Butler, K. S.; Peeler, D. J.; Casey, B. J.; Dair, B. J.; Elespuru, R. K. Silver Nanoparticles: Correlating Nanoparticle Size and Cellular Uptake with Genotoxicity. *Mutagenesis* **2015**, *30*, 577–591.
- (29) Magdolenova, Z.; Collins, A.; Kumar, A.; Dhawan, A.; Stone, V.; Dusinska, M. Mechanisms of Genotoxicity. A Review of in Vitro and in Vivo Studies with Engineered Nanoparticles. *Nanotoxicology* **2014**, *8*, 233–278.
- (30) Greulich, C.; Diendorf, J.; Geßmann, J.; Simon, T.; Habijan, T.; Eggeler, G.; Schildhauer, Ta.; Epple, M.; Köller, M. Cell Type-Specific Responses of Peripheral Blood Mononuclear Cells to Silver Nanoparticles. *Acta Biomater.* **2011**, *7*, 3505–3514.
- (31) Juarez-Moreno, K.; Gonzalez, E.; Girón-Vázquez, N.; Chávez-Santoscoy, R.; Mota-Morales, J.; Perez-Mozqueda, L.; Garcia-Garcia, M.; Pestryakov, A.; Bogdanchikova, N. Comparison of Cytotoxicity and Genotoxicity Effects of Silver Nanoparticles on Human Cervix and Breast Cancer Cell Lines. *Hum. Exp. Toxicol.* **2017**, *36*, 931–948.
- (32) Kalmantaeva, O. V.; Firstova, V. V.; Potapov, V. D.; Zyrina, E. V.; Gerasimov, V. N.; Ganina, E. A.; Burmistrov, V. A.; Borisov, A. V. Silver-Nanoparticle Exposure on Immune System of Mice Depending on the Route of Administration. *Nanotechnol. Russ.* **2014**, *9*, 571–576.
- (33) Semenov, F. V.; Fidarova, K. M. The Treatment of the Patients Presenting with Chronic Inflammation of the Trepanation Cavity with a Preparation Containing Silver Nanoparticles Following Sanitation Surgery of the Open Type. *Vestn. Otorinolaringol.* **2012**, *6*, 117–119.
- (34) Almonaci Hernández, C. A.; Juarez-Moreno, K.; Castañeda Juárez, M. E.; Almanza-Reyes, H.; Pestryakov, A.; Bogdanchikova, N. Silver Nanoparticles for the Rapid Healing of Diabetic Foot Ulcers. *Int. J. Med. Nano Res.* **2017**, *4*, No. 019.
- (35) Glotov, A. G.; Glotova, T. I.; Sergeev, A. A.; Belkina, T. V.; Sergeev, A. N. Antiviral Activity of Different Drugs in Vitro against Viruses of Bovine Infectious Rhinotracheitis and Bovine Diarrhea. *Vopr. Virusol.* **2004**, *49*, 43–46.
- (36) Borrego, B.; Lorenzo, G.; Mota-Morales, J. D.; Almanza-Reyes, H.; Mateos, F.; López-Gil, E.; de la Losa, N.; Burmistrov, V. A.; Pestryakov, A. N.; Brun, A.; et al. Potential Application of Silver Nanoparticles to Control the Infectivity of Rift Valley Fever Virus in Vitro and in Vivo. *Nanomedicine* **2016**, *12*, 1185–1192.
- (37) Bogdanchikova, N.; Vázquez-Muñoz, R.; Huerta-Saquero, A.; Peña-Jasso, A.; Aguilar-Uzcanga, G.; Picos-Díaz, P. L.; Pestryakov, A.; Burmistrov, V. A.; Martynyuk, O.; Luna-Vázquez-Gómez, R.; et al. Silver Nanoparticles Composition for Treatment of Distemper in Dogs. *Int. J. Nanotechnol.* **2016**, *13*, 227–237.
- (38) Juarez-Moreno, K.; Mejía-Ruiz, C. H.; Díaz, F.; Reyna-Verdugo, H.; Re, A. D.; Vázquez-Félix, E. F.; Sánchez-Castrejón, E.; Mota-Morales, J. D.; Pestryakov, A.; Bogdanchikova, N. Effect of Silver Nanoparticles on the Metabolic Rate, Hematological Response, and Survival of Juvenile White Shrimp *Litopenaeus vannamei*. *Chemosphere* **2017**, *169*, 716–724.
- (39) Spinoso-Castillo, J. L.; Chavez-Santoscoy, R. A.; Bogdanchikova, N.; Pérez-Sato, J. A.; Morales-Ramos, V.; Bello-Bello, J. J. Antimicrobial and Hormetic Effects of Silver Nanoparticles on in Vitro Regeneration of Vanilla (*Vanilla planifolia* Jacks. Ex Andrews) Using a Temporary Immersion System. *Plant Cell, Tissue Organ Cult.* **2017**, *129*, 195–207.
- (40) Bello-Bello, J. J.; Chavez-Santoscoy, R. A.; Lecona-Guzmán, C. A.; Bogdanchikova, N.; Salinas-Ruiz, J.; Gómez-Merino, F. C.; Pestryakov, A. Hormetic Response by Silver Nanoparticles on in Vitro Multiplication of Sugarcane (*Saccharum* Spp. Cv. Mex 69-290) Using a Temporary Immersion System. *Dose-Response* **2017**, *15*, 1–9.
- (41) Valenzuela-Salas, L. M.; Girón-Vázquez, N. G.; García-Ramos, J. C.; Torres-Bugarín, O.; Gómez, C.; Pestryakov, A.; Villarreal-Gómez, L. J.; Toledano-Magaña, Y.; Bogdanchikova, N. Antiproliferative and Antitumor Effect of Non-Genotoxic Silver Nanoparticles on Melanoma Models. *Oxid. Med. Cell. Longevity* **2019**, No. 4528241.
- (42) Ochoa-Meza, A. R.; Álvarez-Sánchez, A. R.; Romo-Quinonez, C. R.; Barraza, A.; Magallón-Barajas, F. J.; Chávez-Sánchez, A.; García-Ramos, J. C.; Toledano-Magaña, Y.; Bogdanchikova, N.;

Pestryakov, A.; et al. Silver Nanoparticles Enhance Survival of White Spot Syndrome Virus Infected *Penaeus vannamei* Shrimps by Activation of Its Immunological System. *Fish Shellfish Immunol.* **2019**, *84*, 1083–1089.

(43) Bello-Bello, J.; Spinoso-Castillo, J.; Arano-Avalos, S.; Martínez-Estrada, E.; Arellano-García, M.; Pestryakov, A.; Toledano-Magaña, Y.; García-Ramos, J.; Bogdanchikova, N. Cytotoxic, Genotoxic, and Polymorphism Effects on *Vanilla planifolia* Jacks Ex Andrews after Long-Term Exposure to Argovit Silver Nanoparticles. *Nanomaterials* **2018**, *8*, 754.

(44) OECD. *Guideline for the Testing of Chemicals: Mammalian Erythrocyte Micronucleus Test*, Test No. 474; OECD, 2016.

(45) Evans, H.; O'Riordan, M. Human Peripheral Blood Lymphocytes for the Analysis of Chromosome Aberrations in Mutagen Test. *Mutat. Res., Environ. Mutagen. Relat. Subj.* **1975**, *31*, 135–148.

(46) Souza, T. A. J.; Franchi, L. P.; Rosa, L. R.; da Veiga, M. A. M. S.; Takahashi, C. S. Cytotoxicity and Genotoxicity of Silver Nanoparticles of Different Sizes in CHO-K1 and CHO-XRSS Cell Lines. *Mutat. Res., Genet. Toxicol. Environ. Mutagen.* **2016**, *795*, 70–83.

(47) Bastos, V.; Duarte, I. F.; Santos, C.; Oliveira, H. Genotoxicity of Citrate-Coated Silver Nanoparticles to Human Keratinocytes Assessed by the Comet Assay and Cytokinesis Blocked Micronucleus Assay. *Environ. Sci. Pollut. Res.* **2017**, *24*, 5039–5048.

(48) Xu, L.; Li, X.; Takemura, T.; Hanagata, N.; Wu, G.; Chou, L. L. Genotoxicity and Molecular Response of Silver Nanoparticle (NP)-Based Hydrogel. *J. Nanobiotechnol.* **2012**, *10*, No. 16.

(49) AshaRani, P. V.; Mun, G. L. K.; Hande, M. P.; Valiyaveetil, S. Cytotoxicity and Genotoxicity of Silver Nanoparticles in Human Cells. *ACS Nano* **2009**, *3*, 279–290.

(50) Sordo, M.; Herrera, L. A.; Ostrosky-Wegman, P.; Rojas, E. Cytotoxic and Genotoxic Effects of As, MMA, and DMA on Leukocytes and Stimulated Human Lymphocytes. *Teratog. Carcinog. Mutagen.* **2001**, *21*, 249–260.

(51) Flora, S. J. S. Arsenic-Induced Oxidative Stress and Its Reversibility. *Free Radical Biol. Med.* **2011**, *51*, 257–281.

(52) Yu, H.-S.; Chen, G.-S.; Liao, W.-T.; Chang, K.-L.; Yu, C.-L. Arsenic Induces Tumor Necrosis Factor  $\alpha$  Release and Tumor Necrosis Factor Receptor 1 Signaling in T Helper Cell Apoptosis. *J. Invest. Dermatol.* **2002**, *119*, 812–819.

(53) Liu, S. X.; Davidson, M. M.; Tang, X.; Walker, W. F.; Athar, M.; Ivanov, V.; Hei, T. K. Mitochondrial Damage Mediates Genotoxicity of Arsenic in Mammalian Cells. *Cancer Res.* **2005**, *65*, 3236–3242.

(54) Colognato, R.; Coppède, F.; Ponti, J.; Sabbioni, E.; Migliore, L. Genotoxicity Induced by Arsenic Compounds in Peripheral Human Lymphocytes Analysed by Cytokinesis-Block Micronucleus Assay. *Mutagenesis* **2007**, *22*, 255–261.

(55) Robinson, B. V.; Sullivan, F. M.; Borzelleca, J. F.; Schwartz, S. L. *PVP. A Critical Review of the Kinetics and Toxicology of Polyvinylpyrrolidone (Povidone)*; CRC Press: Chelsea, 1990.

(56) Damjanovic, V.; Thomas, D. The Use of Polyvinylpyrrolidone as a Cryoprotectant in the Freezing of Human Lymphocytes. *Cryobiology* **1974**, *11*, 312–316.

(57) Nair, B. Final Report on The Safety Assessment of Polyvinylpyrrolidone (PVP). *Int. J. Toxicol.* **1998**, *17*, 95–130.

(58) Shimizu, N.; Itoh, N.; Utiyama, H.; Wahl, G. M. Selective Entrapment of Extrachromosomally Amplified DNA by Nuclear Budding and Micronucleation during S Phase. *J. Cell Biol.* **1998**, 1307.

(59) Shimizu, N.; Shimura, T.; Tanaka, T. Selective Elimination of Acentric Double Minutes from Cancer Cells through the Extrusion of Micronuclei. *Mutat. Res., Fundam. Mol. Mech. Mutagen.* **2000**, 81.

(60) Fenech, M. Cytokinesis-Block Micronucleus Assay Evolves into a “Cytome” Assay of Chromosomal Instability, Mitotic Dysfunction and Cell Death. *Mutat. Res., Fundam. Mol. Mech. Mutagen.* **2006**, *600*, 58–66.

(61) Cheong, H. S. J. J.; Seth, I.; Joiner, M. C.; Tucker, J. D. Relationships among Micronuclei, Nucleoplasmic Bridges and Nuclear Buds within Individual Cells in the Cytokinesis-Block Micronucleus Assay. *Mutagenesis* **2013**, *28*, 433–440.

(62) Ahlberg, S.; Antonopoulos, A.; Diendorf, J.; Dringen, R.; Epple, M.; Flöck, R.; Goedecke, W.; Graf, C.; Haberl, N.; Helmlinger, J.; et al. PVP-Coated, Negatively Charged Silver Nanoparticles: A Multi-Center Study of Their Physicochemical Characteristics, Cell Culture and in Vivo Experiments. *Beilstein J. Nanotechnol.* **2014**, *5*, 1944–1965.

(63) Vázquez Muñoz, R. *Evaluación de Las Interacciones Entre Las Nanoparticulas de Plata y Microorganismos Patógenos*; Centro de Investigación Científica y de Educación Superior de Ensenada: Baja California, 2017.

(64) Hadrup, N.; Lam, H. R. Oral Toxicity of Silver Ions, Silver Nanoparticles and Colloidal Silver - A Review. *Regul. Toxicol. Pharmacol.* **2014**, *68*, 1–7.

(65) Swanner, J.; Mims, J.; Carroll, D. L.; Akman, S. A.; Furdui, C. M.; Torti, S. V.; Singh, R. N. Differential Cytotoxic and Radiosensitizing Effects of Silver Nanoparticles on Triple-Negative Breast Cancer and Non-Triple-Negative Breast Cells. *Int. J. Nanomed.* **2015**, *10*, 3937–3953.

(66) Fenech, M. The in Vitro Micronucleus Technique. *Mutat. Res., Fundam. Mol. Mech. Mutagen.* **2000**, *455*, 81–95.

(67) Bartlett, M. S. The Square Root Transformation in Analysis of Variance. *Suppl. J. R. Stat. Soc.* **1936**, *3*, 68.

(68) Brodin, U. Statistical Analysis of the Micronucleus Test - a Modelling Approach Ulf Brodin. *Mutat. Res., Fundam. Mol. Mech. Mutagen.* **1989**, *211*, 259–264.